Three-Level Optimized Pulse Patterns with Zero Common-Mode Voltage

Isavella Koukoula*, Petros Karamanakos*, and Tobias Geyer†
*Faculty of Information Technology and Communication Sciences, Tampere University, Tampere, Finland,
†ABB System Drives, Turgi, Switzerland
Email: *isavella.koukoula@tuni.fi, *p.karamanakos@ieee.org, †t.geyer@ieee.org

***Abstract*—This paper investigates the computation of three-level optimized pulse patterns (OPPs) with zero common-mode voltage (CMV). To do so, a set of linear constraints that guarantee zero CMV is derived, and a systematic way of implementing it is presented. Moreover, to alleviate the increased computational demands of the associated optimization problem, a method that can reduce the computational time of three-level OPPs with zero CMV by up to 99% is proposed. Finally, to mitigate the increased current harmonics due to the CMV elimination, the symmetry requirements of the OPPs are relaxed. In doing so, as shown by the presented numerical results, the current quality can be improved, but alas, only marginally and over a limited range of modulation indices.**

***Index Terms*—Optimized pulse patterns (OPPs), modulation scheme, pulse width modulation (PWM), voltage source converter (VSC), multilevel converter, common-mode voltage.**

I. Introduction

The common-mode voltage (CMV) and its rapid $\mathrm{d}v/\mathrm{d}t$ changes are associated with bearing currents that damage the motor bearings [1]. Additionally, the CMV is the main cause of leakage currents that stress the motor insulation. Therefore, eliminating the CMV can improve the lifetime of the motor.

The idea of *eliminating* the CMV in three-level converters was first presented in [2]. Traditionally, space vector modulation (SVM) uses the three nearest voltage vectors to generate the desired voltage. As shown in [3], by only using the voltage vectors that produce zero CMV, the CMV can be kept zero. In this direction, several SVM techniques have been presented that have different features, such as power losses, switching frequency, distribution of the load, etc. Such methods are characterized by the selection of the voltage vectors used, e.g., three medium vectors (3MV), three medium vectors with 120° disposition (3MV120), or two medium voltage vectors and the zero vector (2MV1Z) [4]. Compared with conventional three-level SVM, all the aforementioned methods increase current distortions as well as the switching events per modulation cycle, thus resulting in higher power losses. At the same time, the dc-link voltage utilization is limited to 78.5%, as the maximum achievable modulation index is $m_{\max} = 1$ (out of $4/\pi$) [5].

To partly mitigate the above disadvantages, an alternative SVM technique is proposed in [6], and [7]. With conventional (continuous) SVM the switching patterns are typically symmetrical with respect to the modulation half-cycle. In these works, however, an asymmetric pattern with twice the sampling frequency is implemented. In doing so, the amount of switching events per modulation cycle does not increase. Additionally, the harmonics are moved to higher frequencies, therefore, improving the harmonic performance.

Despite the improvement achieved with the above-mentioned modulation methods, the pitfalls of SVM-based strategies for zero CMV are still prominent. Optimized pulse patterns (OPPs) can address these issues to a greater extent. This pulse width modulation (PWM) technique can achieve the minimum harmonic distortions by computing the optimal switching angles (i.e., switching time instants) of a pulse pattern for a given modulation index in an offline optimization procedure [8]. Moreover, different objectives can be taken into account by modifying the OPP optimization problem. This feature is used in e.g., [9] and [10] to compute OPPs with limited CMV. More specifically, the former proposes the computation of OPPs with zero CMV. To do so, the switching angles are divided into pairs that are appropriately constrained. This, however, can become very challenging as the dimension of the problem increases (i.e., as the number of switching angles grows). However, these OPPs not only produce lower current distortions per switching frequency compared with the SVM counterparts but also the available voltage is utilized up to 86.6% as the maximum modulation index is $m_{\max} = 2\sqrt{3}/\pi$ (out of $4/\pi$). It is worth noting that this modulation index is the maximum achievable with zero CMV since the long voltage vectors cannot be used.

Contrary to [9], [10] proposes the *partial* elimination of the CMV. More specifically, [10] calculates the exact CMV in the time domain and limits it below a desired value. However, as simultaneous switching in two phases is required to achieve zero CMV, this renders this method unsuitable for CMV complete elimination due to numerical issues associated with this feature. Nevertheless, [10] showed that relaxing the symmetry properties of the OPPs with limited CMV increases the search space, and as a result, a deterioration in the current quality can be avoided.

Motivated by the above, this work proposes the fast computation of three-level OPPs with zero CMV. To do so, a set of linear constraints for the switching angles is derived based on a strategy that identifies *a priori* the relevant constraints. As a result, the proposed strategy can solve the zero-CMV OPP optimization problem by up to 99% faster than the procedure proposed in [9]. Moreover, in line with [10], the symmetry

requirements of the OPP are relaxed to mitigate the increased current harmonics. As shown by the numerical results for a medium-voltage drive, even though this approach adds degrees of freedom to the solution process, it can only marginally improve the harmonic distortions and only over a limited range of modulation indices. This is due to the strict switching requirements for zero CMV that inherently limit the search space.

II. OPPs with Zero Common-Mode Voltage

Assuming a three-level converter with a device switching frequency f_{sw}, the OPP is a 2π–periodic signal $u(\theta) \in \{-1, 0, 1\}$, with a fundamental frequency f_1, where θ is the angle of the pulse pattern. The full-wave switching signal can be described by the $4d$ switching angles α_i, $i \in \{1, \ldots, 4d\}$, where the pulse number d is defined as the ratio $d = f_{\text{sw}}/f_1$. At every switching angle α_i a switching transition $\Delta u_i = u_i - u_{i-1} \in \{-1, 1\}$ occurs.

The OPP is computed by minimizing an objective function that captures the load current total demand distortion (TDD). Assuming an inductive load, the current TDD is given by

$$I_{\text{TDD}} = \frac{1}{\sqrt{2} I_{\text{nom}} \omega_1 L} \frac{V_{\text{dc}}}{2} \sqrt{\sum_{n \neq 1} \left(\frac{\hat{u}_n}{n} \right)^2} = c\sqrt{J}\,. \tag{1}$$

The parameter c in (1) depends on the nominal current I_{nom}, angular fundamental frequency ω_1, load inductance L, and dc-link voltage V_{dc}. Hence, from a mathematical optimization point of view, it can be considered as an offset and it can thus be discarded as it does not affect the optimization result. This means that the objective function J of the OPP problem accounts only for the voltage harmonics $\hat{u}_n$, weighted by their harmonic order. Note that the amplitude of the n^{th} harmonic is given by $\hat{u}_n = \sqrt{a_n^2 + b_n^2}$, with a_n and b_n being the Fourier coefficients of the periodic OPP waveform. For the analytical expressions of the Fourier coefficients, the reader is referred to [11].

A. Traditional OPP Problem

Traditional OPPs have the following properties:

- (P1) Three-phase symmetry, i.e., if the OPP for phase a is $u_a(\theta) = u(\theta)$, then $u_b(\theta) = u\left(\theta - \frac{2\pi}{3}\right)$ and $u_c(\theta) = u\left(\theta + \frac{2\pi}{3}\right)$ are the OPPs for phases b and c, respectively;
- (P2) Half-wave symmetry, i.e., $u(\theta) = -u(\theta + \pi)\ \forall \theta \in [0, \pi]$;
- (P3) Quarter-wave symmetry, i.e., $u(\theta) = u(\pi - \theta)\ \forall \theta \in \left[0, \frac{\pi}{2}\right]$;
- (P4) Unipolar switching, i.e., $u(\theta) \geq 0,\ \forall \theta \in \left[0, \frac{\pi}{2}\right]$, whereas the first switch position is always zero, i.e., $u_0 = 0$.

An OPP with all the above properties, hereafter referred to as quarter- and half-wave symmetric (QaHWS) OPP, can be fully described by using only the d switching angles $\alpha_1, \ldots, \alpha_d \in [0, \pi/2]$ of u_a. Such an OPP is shown in Fig. 1(a). QaHWS OPPs are computed by solving the following nonlinear optimization problem

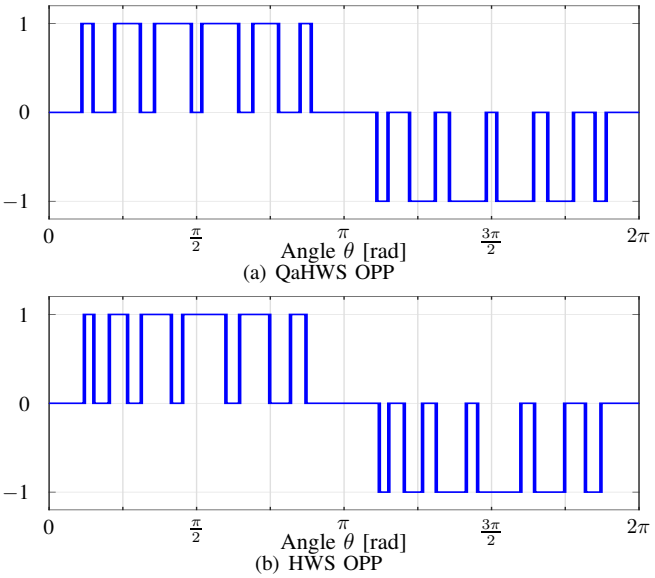

(a) QaHWS OPP

(b) HWS OPP

Fig. 1: Examples of OPPs with different symmetry properties for $d = 6$ at modulation index $m = 0.8$.

$$\begin{aligned} \underset{\boldsymbol{\alpha}_Q}{\text{minimize}} \quad & J_1(\boldsymbol{\alpha}_Q) = \textstyle\sum_{n=5,7,\ldots} \left(\frac{b_n}{n}\right)^2 \\ \text{subject to} \quad & b_1 = m \\ & 0 \leq \alpha_1 \leq \alpha_2 \leq \ldots \leq \alpha_d \leq \tfrac{\pi}{2}\,, \end{aligned} \tag{2}$$

where $\boldsymbol{\alpha}_Q = [\alpha_1\ \alpha_2\ \ldots\ \alpha_d]^T$, and $m \in [0, 4/\pi]$ is the desired modulation index. Note that due to the QaHWS, the a_n Fourier coefficients are zero, while harmonics triplen odd harmonics (i.e., common-mode harmonics) do not drive harmonic current. As a result, only non-triplen, odd harmonics are relevant and are thus considered in the objective function of (2).

B. Common-Mode Voltage

Let v_x denote the output voltage of the inverter in phase x, with $x \in \{a, b, c\}$. The CMV is defined as the average of the three single-phase output voltages. Since it holds that $v_x = \frac{V_{\text{dc}}}{2} u_x$, it directly follows that the *common-mode (CM) switch position* u_o is defined as

$$u_o(\theta) = \frac{u_a(\theta) + u_b(\theta) + u_c(\theta)}{3}\,. \tag{3}$$

The CM switch position u_o is a $\frac{2\pi}{3}$–periodic signal, and inherits the symmetry properties of the OPP. Due to the QaHWS, u_o can be constructed based on the information included in the three-phase OPP $\boldsymbol{u}_{abc}(\vartheta) = [u_a(\vartheta)\ u_b(\vartheta)\ u_c(\vartheta)]^T$ for $\vartheta \in \left[0, \frac{\pi}{6}\right]$, which can be derived from the single-phase OPP $u(\theta)$, $\theta \in \left[0, \frac{\pi}{2}\right]$ as follows:

- $u_a(\vartheta)$ is identical to the first $\frac{\pi}{6}$-segment of $u(\theta)$, see the blue segment in Fig. 2.
- $u_b(\vartheta)$ is identical to the third $\frac{\pi}{6}$-segment of $-u(\theta)$. This means that when a switching transition occurs in $u(\theta)$ at α_i, where $\alpha_i \in \left[\frac{\pi}{3}, \frac{\pi}{2}\right]$, then the opposite switching

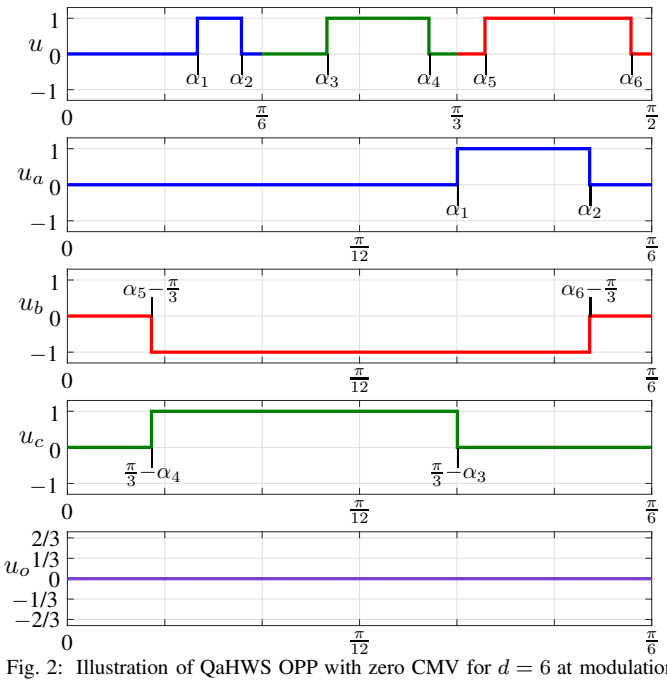

Fig. 2: Illustration of QaHWS OPP with zero CMV for $d = 6$ at modulation index $m = 0.8$

transition happens in u_b at $\alpha_i - \frac{\pi}{3}$, see the red segment in Fig. 2.

- $u_c(\vartheta)$ is identical to the mirrored second $\frac{\pi}{6}$-segment of $u(\theta)$. This means that when a switching transition occurs in $u(\theta)$ at α_i, where $\alpha_i \in \left[\frac{\pi}{6}, \frac{\pi}{3}\right]$, then the mirrored switching transition happens in u_c at $\frac{\pi}{3} - \alpha_i$, see the green segment in Fig. 2.

C. QaHWS OPPs with Zero Common-Mode Voltage

From the above description of the CMV, it is evident that to keep it zero, two phases must switch simultaneously in the opposite direction. Note that due to the unipolar switching see property (P4) in Section II-A), two switching angles α_i, $\alpha_k \in [0, \frac{\pi}{2}]$ correspond to switching transitions $\Delta u_i = \Delta u_k$ if $(i + k) \bmod 2 = 0$.

Based on the above, four cases can be defined depending on which phases switch simultaneously and when, with $\alpha_i \leq \alpha_k$:

- Phases a and b switch simultaneously in the opposite direction if $\alpha_i = \alpha_k - \frac{\pi}{3}$ and $\Delta u_i = \Delta u_k$, see α_2 and α_6 in u—or, equivalently, α_2 in u_a and $\alpha_6 - \frac{\pi}{3}$ in u_b—shown in Fig. 2. This case can be described as $\alpha_k - \alpha_i = \frac{\pi}{3}$ where $\alpha_i \in \left[0, \frac{\pi}{6}\right]$, $\alpha_k \in \left[\frac{\pi}{3}, \frac{\pi}{2}\right]$, and $(i + k) \bmod 2 = 0$.
- Phases b and c switch simultaneously in the opposite direction if $\alpha_k - \frac{\pi}{3} = \frac{\pi}{3} - \alpha_i$ and $\Delta u_i = -\Delta u_k$, see α_4 and α_5 in u—or, equivalently, $\frac{\pi}{3} - \alpha_4$ in u_c and $\alpha_5 - \frac{\pi}{3}$ in u_b—visualized in Fig. 2. This means that this case can be described as $\alpha_k + \alpha_i = \frac{2\pi}{3}$, where $\alpha_i \in \left[\frac{\pi}{6}, \frac{\pi}{3}\right]$, $\alpha_k \in \left[\frac{\pi}{3}, \frac{\pi}{2}\right]$, and $(i + k) \bmod 2 = 1$.
- Phases a and c switch simultaneously in the opposite direction if $\alpha_i = \frac{\pi}{3} - \alpha_k$ and $\Delta u_i = \Delta u_k$, see α_1 and α_3 in u—or α_1 in u_a and $\frac{\pi}{3} - \alpha_3$ in u_c—shown in Fig. 2. Therefore, this case can be described as $\alpha_k + \alpha_i = \frac{\pi}{3}$, where $\alpha_i \in \left[0, \frac{\pi}{6}\right]$, $\alpha_k \in \left[\frac{\pi}{6}, \frac{\pi}{3}\right]$, and $(i + k) \bmod 2 = 0$.

Algorithm 1 Selection of groups of switching angle pairs

```
for each group of switching angle pairs do
    success = 1
    for each switching angle pair {α_i, α_k} in the group do
        Select the possible constraints based on (i + k) mod 2
        if quarter-wave symmetry (see property (P3)) then
            Arrange the switching angles α_i, α_k in their respective π/6-segment
            of u(θ) for the selected constraint
        else
            Arrange the switching angles α_i, α_k in their respective π/3-segment
            of u(θ) for the selected constraint
        end if
        if switching angles are not in ascending order then
            success = 0
            break
        end if
    end for
    if success = 1 then
        Save the derived constraints
    end if
end for
```

- As a corner case, setting $a_k = \frac{\pi}{2}$ in the first two options results in $\alpha_i = \frac{\pi}{6}$, where i can be odd or even. This means that for odd d, there will be one switching angle without a pair that should be set to $\frac{\pi}{6}$.

Based on the cases defined above, the constraints presented in [9] are refined in this work by using the information about the location of each switching angle in a $\frac{\pi}{6}$-segment of $u(\theta)$. With this information, the optimization problem to compute OPPs with zero CMV is formulated as described in the sequel in this section.

First, the d switching angles need to be divided into pairs. There are $d!/(2^{\lfloor \frac{d}{2} \rfloor} \lfloor \frac{d}{2} \rfloor !)$ possible ways to do so. For example, the possible pairs of switching angles for $d = 4$ are

(G1) $\{\alpha_1, \alpha_2\}, \{\alpha_3, \alpha_4\}$
(G2) $\{\alpha_1, \alpha_3\}, \{\alpha_2, \alpha_4\}$
(G3) $\{\alpha_1, \alpha_4\}, \{\alpha_2, \alpha_3\}$

As can be seen, a set of pairs gives rise to what is hereafter referred to as *group* of switching angle pairs, see, e.g., (G1)–(G3).

In a next step, once the groups of pairs are defined, the appropriate constraints are selected. More specifically, for a pair $\{\alpha_i, \alpha_k\}$ the suitable constraints are chosen based on the result of $(i + k) \bmod 2$. Given the cases defined above, there are two possible constraints when $(i + k) \bmod 2 = 0$. This means that multiple constraints correspond to a given group of switching angles. However, not all constraints are relevant. To exemplify this, consider group (G2) from above. For this group, constraints $\alpha_3 - \alpha_1 = \frac{\pi}{3}$ and $\alpha_2 + \alpha_4 = \frac{\pi}{3}$ require $\alpha_1 \in \left[0, \frac{\pi}{6}\right]$, $\alpha_3 \in \left[\frac{\pi}{3}, \frac{\pi}{2}\right]$ and $\alpha_2 \in \left[0, \frac{\pi}{6}\right]$, $\alpha_4 \in \left[\frac{\pi}{6}, \frac{\pi}{3}\right]$. This, in turn, means that $\alpha_4 \leq \alpha_3$, resulting in $\alpha_3 = \alpha_4 = \frac{\pi}{3}$. This, however, implies that one switching transition is skipped, i.e., one pulse is dropped, which subsequently decreases the switching frequency, and thus increases the current TDD. As such behavior is not desired, all sets of equality constraints that cannot be met with the switching angles in ascending order $\alpha_1 < \alpha_2 < \ldots < \alpha_d$ are discarded a priori according to the procedure described in Algorithm 1.

TABLE I: Equality constraints that need to be evaluated for QaHWS OPPs

d	Total constraints	Constraints after selection
2	1	1
3	4	3
4	6	4
5	30	6
6	42	8
7	312	20
8	456	38
9	4,200	66
10	6,120	128
11	69,120	288
12	101,520	716

As can be understood from the above, multiple constraints achieve zero CMV. This implies that the corresponding optimization problem

$$\begin{aligned} \underset{\boldsymbol{\alpha}_Q}{\text{minimize}} \quad & J_1(\boldsymbol{\alpha}_Q) = \textstyle\sum_{n=5,7,\dots} \left(\frac{b_n}{n}\right)^2 \\ \text{subject to} \quad & b_1 = m \\ & 0 \le \alpha_1 \le \alpha_2 \le \ldots \le \alpha_d \le \tfrac{\pi}{2} \\ & \boldsymbol{A}_{\text{eq}}\boldsymbol{\alpha}_Q - \boldsymbol{b}_{\text{eq}} = \boldsymbol{0}\,, \end{aligned} \tag{4}$$

needs to be solved multiple times for a given pulse number d, i.e., once for each one of the different equality constraints. Taking $d = 4$ and group (G2) as an example, one set of relevant constraints includes $\alpha_1 + \alpha_3 = \frac{\pi}{3}$ and $\alpha_4 - \alpha_2 = \frac{\pi}{3}$. Therefore the corresponding equality constraints in problem (4) are

$$\boldsymbol{A}_{\text{eq}} = \begin{bmatrix} 1 & 0 & 1 & 0 \\ 0 & -1 & 0 & 1 \end{bmatrix}, \ \boldsymbol{b}_{\text{eq}} = \begin{bmatrix} \frac{\pi}{3} \\ \frac{\pi}{3} \end{bmatrix}. \tag{5}$$

The number of relevant equality constraints that need to be evaluated (i.e., the number of optimization problems that need to be solved) is shown in Table I.

In a last step, the global optimal solution is found in a post-processing stage by assessing the solutions obtained when solving (4) for the different constraints.

D. OPPs with Symmetry Relaxation

As recently shown in [10], relaxing the OPP symmetry properties helped mitigate the increase in the current TDD caused by the CMV limitation. This is thanks to the increased search space of the three-level OPP problem. Motivated by this, in this work, we relax the symmetry property (P3). By doing so, only half-wave symmetric (HWS) OPPs are considered, meaning that $2d$ switching angles need to be computed, as opposed to the d angles computed for QaHWS OPPs, see problem (2). An example of HWS OPP is depicted in Fig. 1(b).

Considering the symmetry properties of HWS OPPs, the necessary information to compute $\boldsymbol{u}_{abc}(\vartheta), \vartheta \in \left[0, \frac{\pi}{3}\right]$ is included in the single-phase OPP $u(\theta)$ for $\theta \in [0, \pi]$ as the following hold:

- $u_a(\vartheta)$ is identical to the first $\frac{\pi}{3}$-segment of $u(\theta)$, see the blue segment in Fig. 3.
- $u_b(\vartheta)$ is identical to the second $\frac{\pi}{3}$-segment of $-u(\theta)$. Therefore, when a switching transition occurs in $u(\theta)$ at α_i, where $\alpha_i \in \left[\frac{\pi}{3}, \frac{2\pi}{3}\right]$, then the opposite switching transition happens in u_b at $\alpha_i - \frac{\pi}{3}$, see the red segment in Fig. 3.
- $u_c(\vartheta)$ is identical to the third $\frac{\pi}{3}$-segment of $u(\theta)$. Hence, when a switching transition occurs in $u(\theta)$ at α_i, where $\alpha_i \in \left[\frac{2\pi}{3}, \pi\right]$, then the same switching transition happens in u_c at $\alpha_i - \frac{2\pi}{3}$, see the green segment in Fig. 3.

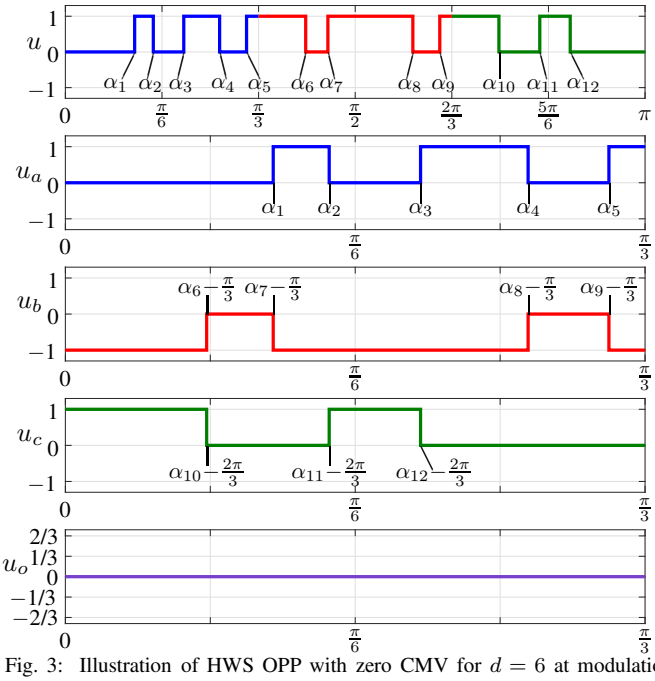

Fig. 3: Illustration of HWS OPP with zero CMV for $d = 6$ at modulation index $m = 0.8$.

The angle constraints for the case of HWS OPPs can be derived by following a similar approach to that for QaHWS OPPs. This means that, as previously, different cases are defined based on which phases switch simultaneously with $\alpha_i \le \alpha_k$, i.e.,

- Phases a and b switch simultaneously in the opposite direction if $\alpha_i = \alpha_k - \frac{\pi}{3}$ and $\Delta u_i = \Delta u_k$, see α_1 and α_7—or, equivalently, α_1 in u_a and $\alpha_7 - \frac{\pi}{3}$ in u_b—in Fig. 3. Hence, this case can be described as $\alpha_k - \alpha_i = \frac{\pi}{3}$, where $\alpha_i \in \left[0, \frac{\pi}{3}\right]$, $\alpha_k \in \left[\frac{\pi}{3}, \frac{2\pi}{3}\right]$, and $(i + k) \bmod 2 = 0$.
- Phases b and c switch simultaneously in the opposite direction if $\alpha_i - \frac{\pi}{3} = \alpha_k - \frac{2\pi}{3}$ and $\Delta u_i = \Delta u_k$, see α_6 and α_{10}—or $\alpha_6 - \frac{\pi}{3}$ in u_b and $\alpha_{10} - \frac{2\pi}{3}$ in u_c—in Fig. 3. Thus, this case corresponds to $\alpha_k - \alpha_i = \frac{\pi}{3}$, where $\alpha_i \in \left[\frac{\pi}{3}, \frac{2\pi}{3}\right]$, $\alpha_k \in \left[\frac{2\pi}{3}, \pi\right]$, and $(i + k) \bmod 2 = 0$.
- Phases a and c switch simultaneously in the opposite direction if $\alpha_i = \alpha_k - \frac{2\pi}{3}$ and $\Delta u_i = -\Delta u_k$, see α_2 and α_{11}—or α_2 in u_a and $\alpha_{11} - \frac{2\pi}{3}$ in u_c—in Fig. 3. This means this case is governed by $\alpha_k + \alpha_i = \frac{2\pi}{3}$, where $\alpha_i \in \left[0, \frac{\pi}{3}\right]$, $\alpha_k \in \left[\frac{2\pi}{3}, \pi\right]$ and $(i + k) \bmod 2 = 1$.

As with QaHWS OPPs, to reformulate the optimization problem the $2d$ switching angles need to be divided into pairs. There are $(2d)!/(2^d d!)$ possible ways to do so. Subsequently, the constraints are selected for each group of switching angle pairs. Note that there is only one possible constraint $\alpha_k - \alpha_i = \frac{\pi}{3}$ for a pair $\{\alpha_i, \alpha_k\}$ with $(i + k) \bmod 2 = 0$,

TABLE II: Equality constraints that need to be evaluated for HWS OPPs

d	Total constraints	Constraints after selection
2	3	2
3	15	6
4	105	23
5	945	97
6	10,395	513

but, at the same time, two ways of arranging the switching angles in $u(\theta)$, i.e., (a) $\alpha_i \in \left[0, \frac{\pi}{3}\right]$ and $\alpha_k \in \left[\frac{\pi}{3}, \frac{2\pi}{3}\right]$, or (b) $\alpha_i \in \left[\frac{\pi}{3}, \frac{2\pi}{3}\right]$ and $\alpha_k \in \left[\frac{2\pi}{3}, \pi\right]$. This means that the final number of constraints is equal to the number of groups of switching angle pairs, significantly increasing the complexity of the zero-CMV HWS OPP problem.

Notwithstanding the foregoing, not all the resulting constraints are relevant. Therefore, similar to the QaHWS OPPs case, the relative location of the switching angles in $u(\theta)$ is used to discard all constraints that lead to pulse dropping. To do so, the procedure described in Algorithm 1 is adopted. Note that even though this procedure is similar to the case of QaHWS OPPs, the constraints are different. Moreover, for QaHWS OPPs the first $\frac{\pi}{2}$-segment of $u(\theta)$ is divided into three $\frac{\pi}{6}$-segments, whereas the first π-segment of HWS $u(\theta)$ is divided into three $\frac{\pi}{3}$-segments.

Given the above, the number of relevant equality constraints that need to be evaluated for HWS OPPs is shown in Table II. Based on these constraints, the optimization problem that needs to be solved for each set of constraints to compute HWS OPPs with zero CMV is

$$\begin{aligned} \underset{\boldsymbol{\alpha}_H}{\text{minimize}} \quad & J_1(\boldsymbol{\alpha}_H) = \textstyle\sum_{n=5,7,\ldots} \frac{a_n^2+b_n^2}{n^2} \\ \text{subject to} \quad & a_1 = 0,\ b_1 = m \\ & 0 \leq \alpha_1 \leq \alpha_2 \leq \ldots \leq \alpha_{2d} \leq \pi \\ & \boldsymbol{A}_{\text{eq}}\boldsymbol{\alpha}_H - \boldsymbol{b}_{\text{eq}} = \boldsymbol{0}\,, \end{aligned} \tag{6}$$

where $\boldsymbol{\alpha}_H = [\alpha_1\ \alpha_2\ \ldots\ \alpha_{2d}]^T$. Note that due to the HWS, both a_n and b_n Fourier coefficients are nonzero for the non-triplen, odd harmonics, except for the fundamental component, where it is desired that $a_1 = 0$ such that the phase of the fundamental component is zero.

III. Numerical Results

In this section, the optimization results for (a) traditional QaHWS OPPs (see problem (2)); (b) QaHWS with zero CMV (see problem (4)), and (c) HWS OPPs with zero CMV (see (6)) are presented. OPPs in the (b) category are hereafter referred to as QaHWS CMZ OPPs, while those in category (c) as HWS CMZ OPPs. All OPPs are computed for a medium-voltage (MV) drive system, i.e., a three-level inverter with a dc-link voltage of $V_{\text{dc}} = 5.2\,\text{kV}$ that drives a 3.3 kV, 50 Hz squirrel-cage induction machine with rated current 2.12 kA current and total leakage reactance of 0.255 per unit (p.u.). For demonstration purposes, OPPs with $d = 4$, 5, and 6 are considered, see Figs. 4 to 6.

As can be seen in all cases examined, the maximum modulation index is $m_{\max} = 1.1$ when the CMV is eliminated. The available dc-link voltage cannot be fully utilized, since the long voltage vectors result in nonzero CMV. Moreover, the

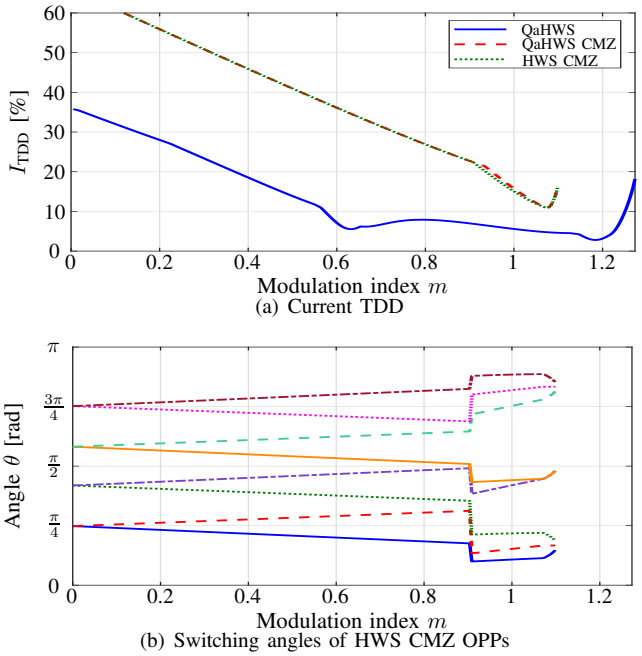

(a) Current TDD

(b) Switching angles of HWS CMZ OPPs

Fig. 4: QaHWS and HWS OPPs for $d = 4$ without and with the CMV constraint. The solid (blue) line corresponds to the traditional QaHWS OPPs, the dashed (red) line to QaHWS OPPs with zero CMV (QaHWS CMZ OPPs), and the dotted (green) line to HWS OPPs with zero CMV (HWS CMZ OPPs).

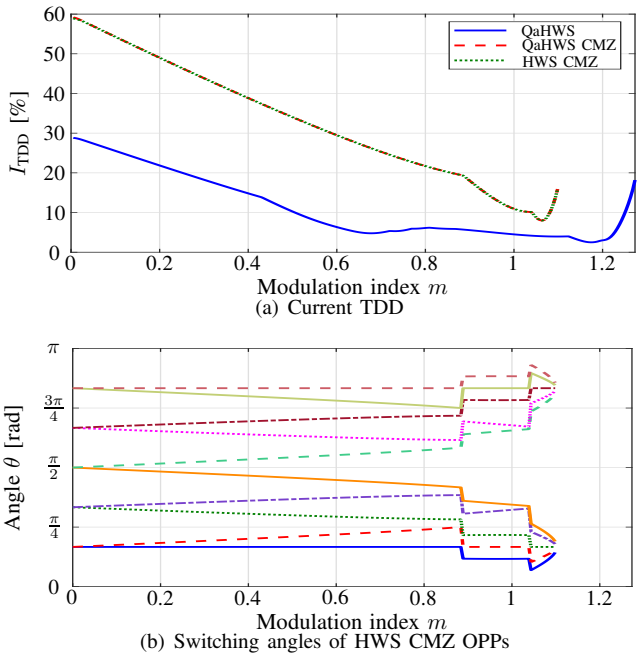

(a) Current TDD

(b) Switching angles of HWS CMZ OPPs

Fig. 5: QaHWS and HWS OPPs for $d = 5$ without and with the CMV constraint. The solid (blue) line corresponds to the traditional QaHWS OPPs, the dashed (red) line to QaHWS OPPs with zero CMV (QaHWS CMZ OPPs), and the dotted (green) line to HWS OPPs with zero CMV (HWS CMZ OPPs).

elimination of the CMV occurs at a cost of an increased current TDD, as can be observed in Figs. 4(a) to 6(a). Nevertheless, it is worth noting that for pulse numbers $d = 4$ and 6, relaxing the quarter-wave symmetry (i.e., property (P3) in Section II-A) leads to slightly improved results compared to QaHWS CMZ OPPs. This can be observed in the modulation index range $0.90 \leq m \leq 1.07$ for pulse number $d = 4$,

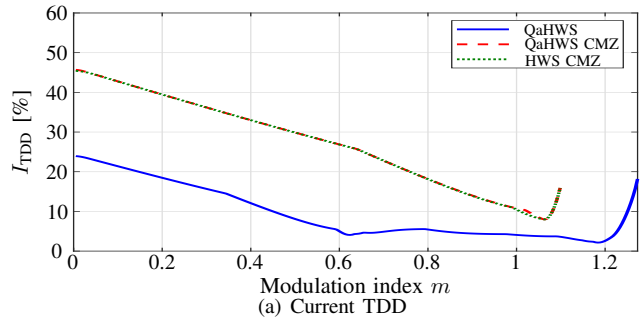

(a) Current TDD

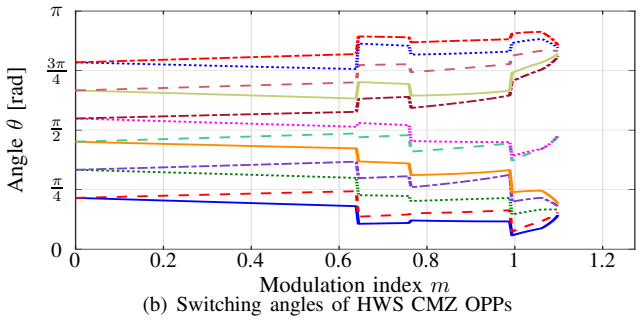

(b) Switching angles of HWS CMZ OPPs

Fig. 6: QaHWS and HWS OPPs for $d = 6$ without and with the CMV constraint. The solid (blue) line corresponds to the traditional QaHWS OPPs, the dashed (red) line to QaHWS OPPs with zero CMV (QaHWS CMZ OPPs), and the dotted (green) line to HWS OPPs with zero CMV (HWS CMZ OPPs).

and in the modulation index range $0.76 \leq m \leq 1.06$ for pulse number $d = 6$, where the OPPs do not exhibit QaHWS, see Figs. 4(b) and 6(b). Nevertheless, this difference in the current TDD is minute when the CMV-constrained OPPs are benchmarked against traditional QaHWS OPPs. As shown, a significant increase in I_{TDD} caused by the elimination of CMV is unavoidable, with the TDD of the zero-CMV OPPs being two to five times greater than that of the traditional ones. This implies that relaxing the QaHWS not only increased the computational burden by up to 64 times for $d = 6$ (compare Tables I and II), but also provided almost no benefit.

Nevertheless, despite the unavoidable increase in the current TDD, zero CMV may be still desirable in several applications. Hence, OPPs with zero CMV can be considered the best option for such cases as they compromise the current TDD the least, while they are utilizing the dc-link voltage to the greatest—physically possible—degree. With this in mind, the proposed systematic approach to compute OPPs with zero CMV presented can be beneficial. Specifically, thanks to the presented methodology the computation of, e.g., QaHWS CMZ OPPs can become significantly faster. More specifically, by only selecting the relevant equality constraints, the OPP problem needs to be solved significantly fewer times, while still guaranteeing optimality. Thanks to this, when comparing with the approach proposed in [9], the computational time can be reduced up to 99% for $d = 12$, see Table III.

IV. Conclusions

This paper presented the computation of three-level OPPs with zero CMV. Considering the benefits attributed to zero CMV, a systematic method was presented that allows computing zero-CMV OPPs significantly faster than the existing solution, e.g., the computational time can be decreased by more than 90% when high pulse numbers are concerned. Moreover, both QaHWS and HWS OPPs were considered, and the associated features were assessed. As shown, relaxing the quarter-wave symmetry leads to only a marginal decrease in the current TDD, indicating that HWS OPPs do not offer significant benefits. Considering that HWS OPPs are more computationally demanding to compute, it can be concluded that QaHWS OPPs are the best option.

TABLE III: Reduction in computational time of QaHWS CMZ OPPs with the proposed method

d	Speedup [%]
3	25.00
4	33.33
5	80.00
6	80.95
7	93.59
8	91.67
9	98.43
10	97.91
11	99.58
12	99.29

Acknowledgment

This work was supported in part by ABB Oy Drives and in part by the Academy of Finland.

References

[1] A. Mütze and A. Binder, "Don't lose your bearings—Mitigation techniques for bearing currents in inverter-supplied drive systems," *IEEE Ind. Appl. Mag.*, vol. 12, no. 4, pp. 22–31, Jul./Aug. 2006.

[2] K. Ratnayake and Y. Murai, "A novel PWM scheme to eliminate common-mode voltage in three-level voltage source inverter," in *Proc. IEEE Power Electron. Spec. Conf.*, Fukuoka, Japan, May 1998, pp. 269–274.

[3] H. Zhang, A. Von Jouanne, S. Dai, A. Wallace, and F. Wang, "Multilevel inverter modulation schemes to eliminate common-mode voltages," *IEEE Trans. Ind. Appl.*, vol. 36, no. 6, pp. 1645–1653, Nov. 2000.

[4] M. C. Cavalcanti, A. M. Farias, K. C. Oliveira, F. A. S. Neves, and J. L. Afonso, "Eliminating leakage currents in neutral point clamped inverters for photovoltaic systems," *IEEE Trans. Ind. Electron.*, vol. 59, no. 1, pp. 435–443, Jan. 2012.

[5] L. Kai, J. Zhao, W. Wu, M. Li, L. Ma, and G. Zhang, "Performance analysis of zero common-mode voltage pulse-width modulation techniques for three-level neutral point clamped inverters," *IET Power Electron.*, vol. 9, no. 14, pp. 2654–2664, Nov. 2016.

[6] T.-K. T. Nguyen, N.-V. Nguyen, and N. R. Prasad, "Novel eliminated common-mode voltage PWM sequences and an online algorithm to reduce current ripple for a three-level inverter," *IEEE Trans. Power Electron.*, vol. 32, no. 10, pp. 7482–7493, Oct. 2017.

[7] T.-K. T. Nguyen and N.-V. Nguyen, "An efficient four-state zero common-mode voltage PWM scheme with reduced current distortion for a three-level inverter," *IEEE Trans. Ind. Electron.*, vol. 65, no. 2, pp. 1021–1030, Feb. 2018.

[8] G. S. Buja and G. B. Indri, "Optimal pulsewidth modulation for feeding ac motors," *IEEE Trans. Ind. Appl.*, vol. IA-13, no. 1, pp. 38–44, Jan. 1977.

[9] I. Tsoumas, "On the computation of optimized pulse patterns with zero common mode voltage," in *Proc. Eur. Conf. on Power Electron. and Applicat.*, Genova, Italy, Sep. 2019, pp. P.1–P.10.

[10] I. Koukoula, P. Karamanakos, and T. Geyer, "Three-level optimized pulse patterns with reduced common-mode voltage," in *Proc. IEEE Energy Convers. Congr. Expo.*, Detroit, MI, USA, Oct. 2022, pp. 1–8.

[11] A. Birth, T. Geyer, H. d. T. Mouton, and M. Dorfling, "Generalized three-level optimal pulse patterns with lower harmonic distortion," *IEEE Trans. Power Electron.*, vol. 35, no. 6, pp. 5741–5752, Jun. 2020.